RSC Advances

COMMUNICATION

View Article Online
View Journal | View Issue

Cite this: *RSC Adv.*, 2014, **4**, 41654

Received 22nd May 2014
Accepted 21st August 2014

DOI: 10.1039/c4ra04826a

www.rsc.org/advances

Hydrogenated black ZnO nanoparticles with enhanced photocatalytic performance†

Ting Xia,[a] Petra Wallenmeyer,[a] Alicia Anderson,[a] James Murowchick,[b] Lei Liu*[c] and Xiaobo Chen*[a]

Following our previous findings on hydrogenated black TiO_2 nanoparticles, here, we would like to present our exciting findings on hydrogenated black ZnO nanoparticles, which have displayed long-wavelength absorption and excellent photocatalytic performance. This further demonstrates that hydrogenation is a powerful tool to enhance the optical and photocatalytic performance of nanomaterials.

Hydrogenation has been demonstrated in successfully modifying the structural, electronic and optical properties of TiO_2 nanoparticles, along with its improved photocatalytic performance.[1,2] In our original study, hydrogenated black TiO_2 nanoparticles were obtained by heating white crystalline TiO_2 nanocrystals in a high-pressure pure hydrogen environment.[1a] This treatment induced a thin disordered layer near the surface, surrounding a crystalline core.[1a–d] This layer was believed to introduce extra electronic states in the bandgap and the long-wave length absorption. The hydrogenated black TiO_2 nanoparticles showed excellent and stable photocatalytic performance in photocatalytic hydrogen generation and pollutant (methylene blue and phenol) decomposition.[1a–d] The enhancement was partially attributed to the efficient electron and hole trapping in the disordered layer to allow better charge separation on the surface. Hydrogenated black TiO_2 nanoparticles have also been developed with other fabrication approaches as well, such as electrochemical hydrogenation[2f,g] and hydrogen plasma.[2h] So far, hydrogenated TiO_2 nanocrystals have displayed superior performance in lithium-ion battery,[3] supercapacitor,[4a] fuel cell,[4b] field emission,[4c] and microwave absorption,[4d] besides the excellent photocatalytic performance.

On the other hand, ZnO has also attracted tremendous interests as a semiconductor material for applications in piezotronics,[5a–c] electrochromics,[5d] solar cells,[5e] photocatalysis, *etc.* ZnO is a large bandgap semiconductor material, with a bulk bandgap of 3.2 eV.[5] This large bandgap limits its overall efficiency in photocatalytic application due to its absorption of sunlight only in the ultraviolet (UV) region, which is less than 5% of the entire solar spectrum. Hereby, we demonstrate that by treating white ZnO nanoparticles with hydrogen, hydrogenated black ZnO nanoparticles with long-wavelength absorption can be successfully synthesized, and they have showed much better performance in photocatalytic decomposition of methylene blue than pure ZnO nanoparticles.

Pristine ZnO nanoparticles were prepared from a precursor solution consisting of sodium hydroxide, zinc acetate, ethanol and water.[5f] In a typical synthesis, 5 mmol zinc acetate dissolved in 50 mL ethanol was mixed with 7 mmol sodium hydroxide dissolved in 50 mL ethanol at 0 °C. The white sol was filtered, washed and dried overnight at 120 °C to obtain pristine ZnO nanoparticles. Hydrogenated ZnO nanoparticles (H-ZnO) were obtained by heating pristine ZnO nanoparticles under hydrogen atmosphere, *e.g.* at 400 °C for 2 h. Fig. 1A shows the XRD patterns of pristine and hydrogenated ZnO nanoparticles.

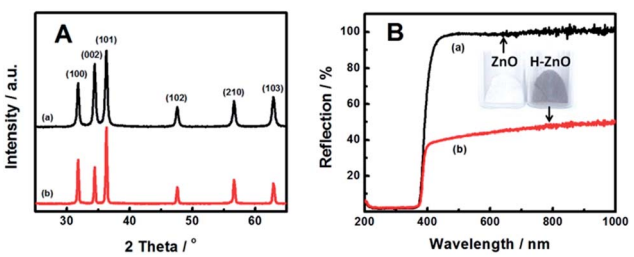

Fig. 1 (A) XRD patterns and (B) UV-visible reflectance spectra of (a) pristine, (b) hydrogenated ZnO nanoparticles.

[a]*Department of Chemistry, University of Missouri – Kansas City, Kansas City, Missouri 64110, USA*

[b]*Department of Geosciences, University of Missouri – Kansas City, Kansas City, MO 64110, USA*

[c]*State Key Laboratory of Luminescence and Applications, Changchun Institute of Optics, Fine Mechanics and Physics, Chinese Academy of Sciences, Changchun, 130033, People's Republic of China. E-mail: chenxiaobo@umkc.edu; liulei@ciomp.ac.cn*

† Electronic supplementary information (ESI) available. See DOI: 10.1039/c4ra04826a

Clearly, both samples were highly crystalline, as seen from their strong diffraction peaks.[5g] The average crystalline grain size can be calculated using the Scherrer equation: $\tau = (K\lambda)/(\beta \cos \theta)$, where τ is the mean size of the ordered (crystalline) domains, which may be smaller then or equal to the grain size, K is the shape factor with a typical value of 0.9, λ is the X-ray wavelength, β is the line broadening full width at half maximum (FWHM) peak height in radians, and θ is the Bragg angle.[6] The average crystalline grain size of pristine and hydrogenated ZnO nanoparticles was 14.3 and 18.8 nm, respectively. For comparison, we also heated pristine ZnO nanoparticles in air (calcined ZnO), and found their average crystalline grain size was 19.1 nm from XRD analysis (Fig. S1†). As the average sizes of the crystalline phase of both hydrogenated and calcined ZnO nanoparticles were much larger than pristine ZnO nanoparticles, the crystalline grain growth of ZnO nanoparticles seemed to be caused by heating at high temperature. Meanwhile, the average size of the crystalline grains in the hydrogenated ZnO nanoparticles was slightly smaller than calcined ZnO nanoparticles. This suggested that some disordered phase was likely formed on the outside of the crystalline phases of ZnO nanoparticles after hydrogenation. This was consistent with our previous study of hydrogenated black TiO_2 nanoparticles,[1a,b] where hydrogenation caused the outer layer of the nanocrystals to become disordered.

Fig. 1B shows the UV-visible spectra of pristine and hydrogenated ZnO nanoparticles. Pristine ZnO nanoparticles were white and reflected 94% of light in the region of 400–1000 nm back, and started to absorb light around 400 nm. The optical bandgap was around 3.2 eV (391 nm at 50% reflection point). Hydrogenated ZnO nanoparticles showed less than 45% reflection in the region of 400–1000 nm (>55% black), and absorbed all light below 400 nm. Absorption in the visible-light region for hydrogenated ZnO nanoparticles seemed to be related to the oxygen defects created by the heating and the incorporation of hydrogen in the ZnO lattice during hydrogenation.[7,8] Losing oxygen atoms in oxide materials are commonly seen by heating at high temperatures, leading to the creation of oxygen defects.[7] Hydrogen can exclusively act as a shallow donor and be responsible for the n-type behavior of ZnO.[8] Interstitial hydrogen (H_i) can be incorporated in a bond-centered configuration and an antibonding orientation,[8a] while substitutional hydrogen occupying an oxygen substitutional site (H_o) accounts for the n-type conductivity and has high thermal stability.[8b] Oxygen vacancies in ZnO are deep level defects, and the hydrogen atoms in ZnO are easily trapped in the oxygen vacancies to form H_o.[8b,d] Thus the large absorption in the visible light region was possibly due to deep oxygen vacancy defects involved with hydrogen in these hydrogenated ZnO nanoparticles, while the absorption in the UV region was likely from the bulk.

The microstructure and crystallinity of the pristine and hydrogenated ZnO nanoparticles were analyzed with transmission electron microscopy (TEM). As shown in Fig. 2A, the average size of the pristine ZnO nanoparticles was around 12–16 nm. This matched well with the size of their average crystalline grains calculated from XRD data, and suggested that the

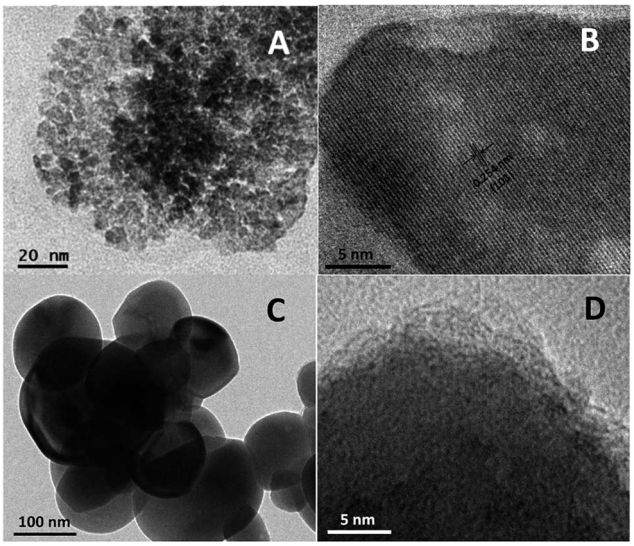

Fig. 2 TEM images of pristine (A) and (B) and hydrogenated (C) and (D) ZnO nanoparticles.

pristine ZnO nanoparticles were most likely single crystalline. The high-resolution TEM (HRTEM) in Fig. 2B further shows well-resolved lattice fringes with a distance of 0.254 nm between the adjacent (101) planes of the wurtzite-type ZnO nanoparticle[5g] and its single crystalline nature. The average size of the hydrogenated ZnO nanoparticles was 150 nm as shown in Fig. 2C. From XRD analysis, the average crystalline grain size of hydrogenated ZnO nanoparticles based on XRD results was 18.8 nm only. This difference on the size suggested that hydrogenated ZnO nanoparticles were made of smaller crystalline grain-sized nanoparticles, likely from the aggregation of ZnO nanoparticles during the hydrogenation treatment. However, this aggregation was likely due to the heating effect in the hydrogenation process, as the TEM analysis of the calcined ZnO nanoparticles had similar average particle size of around 180 nm (Fig. S2A†). The HRTEM of hydrogenated ZnO nanoparticles in Fig. 2D did not reveal clear lattice fringes, suggesting that amorphous/disordered phases existed in the hydrogenated ZnO nanoparticles. Defects are commonly observed along the grain boundaries in crystals.[1a,b,6c] On the other hand, heating ZnO nanoparticles in air induced highly crystallized lattice with well resolved lattice fringes under HRTEM analysis (Fig. S2B†). So, overall, hydrogenation treatment caused the formation of disordered phases in hydrogenated ZnO nanoparticles. This was consistent with the findings in hydrogenated TiO_2 nanoparticles.[1a–c] Such structural disorders could contribute to the long-wavelength absorption in visible-light region of the hydrogenated ZnO nanoparticles.

The existence of the disordered phase in the hydrogenated ZnO nanoparticles was also supported by the results from Raman measurements (Fig. 3A). Pristine ZnO nanoparticles showed clear and sharp Raman peaks at around 115, 228, 350, 459, 697, 969, 1136, and 1479 cm^{-1}, due to the $E_{2,low}$, 2TA (A_1) ($2E_{2,low}$), A_1 (E_2, E_1), E_2,high, A_1 (2TO), A_1 (TO + LO), A_1 (LO) and $2E_1$ (LO) vibrational modes, respectively.[8d,9a] The sharp Raman

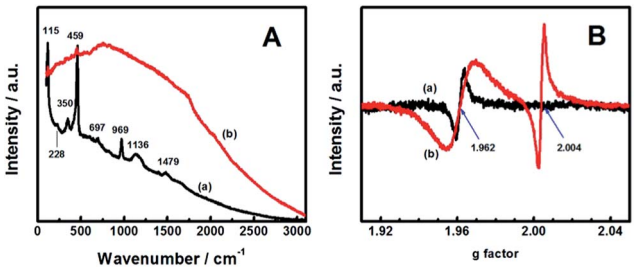

Fig. 3 (A) Raman and (B) ESR spectra of (a) pristine and (b) hydrogenated ZnO nanoparticles.

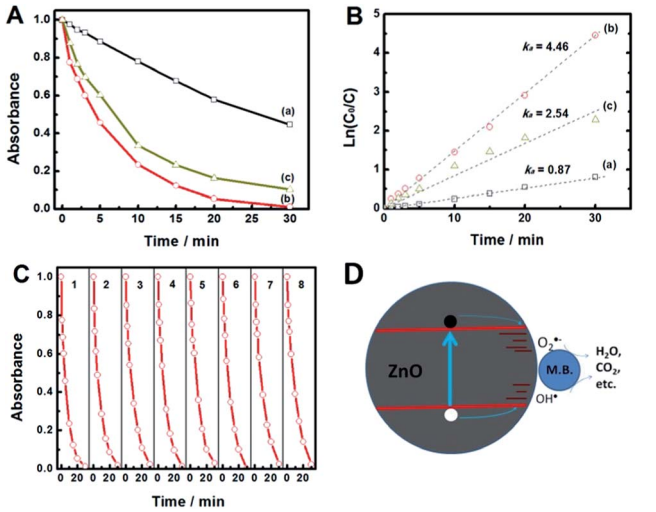

Fig. 4 Comparison of (A) the time profile and (B) $\ln(C_0/C)$ of methylene blue decomposition with (a) pristine and (b) hydrogenated ZnO nanoparticles, in comparison with (c) Degussa P25, a standard catalyst. The *y* axis represents the optical density of the methylene blue solution, whereas the *x* axis is the solar light irradiation time. (C) Cycling tests of solar-driven photocatalytic activity in methylene blue decomposition with hydrogenated ZnO nanoparticles. (D) Proposed mechanism for the improved photocatalytic activity of hydrogenated ZnO nanoparticles on methylene blue decomposition.

peaks meant that the ZnO nanoparticles were well crystalline. Meanwhile, a luminescent background was also observed. This background was likely due to the defects in the ZnO nanoparticles. Hydrogenated ZnO nanoparticles only had weak Raman peaks at around 115 and 459 cm^{-1}, but a much larger luminescent background. The weak Raman peaks and large background suggested that there were a large number of defects in the hydrogenated ZnO nanoparticles. Large luminescence background in the Raman spectrum due to defects has been observed previously in hydrogenated TiO_2 nanoparticles and TiO_2 nanoparticles with oxygen vacancies.[9b] So, similar assignment of the luminescence background is reasonable.

The existence of the defects was examined with electron spin resonance (ESR) spectroscopy. Pristine ZnO nanoparticles had a smaller signal at $g = 1.962$, while hydrogenated ZnO nanoparticles showed a larger signal at $g = 1.962$ and an apparent signal at $g = 2.004$ (Fig. 3B). The signal with a *g*-factor at about 1.962 is generally attributed to the shallow donor, and usually assigned to a singly ionized oxygen vacancy defect, but sometimes attributed to unpaired electrons trapped at oxygen vacancies and even attributed to free carriers in the conduction band.[10] The signal in the ESR spectrum with a *g*-factor close to $g = 2.004$ is commonly attributed to a Zn vacancy.[10] Apparently, hydrogenated ZnO nanoparticles had large amount of zinc vacancy defects, besides more oxygen vacancy defects than the pristine ZnO nanoparticles had. Combined with their UV-visible reflectance spectra, this suggested that the increase of oxygen vacancy defects did not cause apparent light absorption in the visible light region, but the large absorption in the visible-light region of the hydrogenated ZnO nanoparticles might also be due to the co-existence of zinc and oxygen vacancy defect.

The photocatalytic activity was studied with the decomposition of methylene blue under simulated sunlight irradiation. The solar simulator had a 150 watt Xe lamp with an AM 1.5 air mass filter. 1.0 mg of catalyst was added into 3.0 mL methylene blue solution (optical density of 1.0). The UV-vis absorption spectrum of methylene blue was monitored at 664 nm over time after the photocatalytic reaction started. The contribution of the adsorption was removed after stirring the samples in the dark for 30 min before the photocatalytic reaction. Fig. 4A shows the comparison of the solar-driven photocatalytic activity of pristine and hydrogenated ZnO nanoparticles under the same experimental conditions, along with the comparison with Degussa P25, a standard catalyst. After 30 min irradiation, 55% of methylene blue was decomposed with pristine ZnO nanoparticles, and 97% for hydrogenated ZnO nanoparticles, compared to 87% for Degussa P25. The hydrogenated ZnO nanoparticles had better performance over the Degussa P25. When the initial concentration of dye is very small, the degradation of dyes can be described by an apparent first-order equation with a simplified Langmuir–Hinshelwood model: $\ln(C_0/C) = k_a t$, where C_0 is the initial concentration of dye, C is the concentration of the dye, k_a is the apparent first-order rate constant, and t is the illumination time.[11] The rate constants k_a was 0.87 and 4.46 for pristine and hydrogenated ZnO nanoparticles, respectively, compared to 2.54 for P25 (Fig. 4B), given the time unit of 30 min. Therefore, the photocatalytic activity of ZnO nanoparticles was improved 512% by hydrogenation treatment. Meanwhile, hydrogenated ZnO nanoparticles showed good stability in cyclic photocatalytic decomposition of methylene blue as shown in Fig. 4C. No apparent activity decrease was observed. This suggested the excellent stability of the photocatalytic performance of the hydrogenated ZnO nanoparticles. The improved photocatalytic performance was likely related to the co-existence of zinc vacancy defects and the structurally disordered layer which were beneficial for charge trapping and photocatalytic reactions and the long-wavelength absorption.[1] Fig. 4D illustrates the proposed mechanism of the photocatalytic decomposition of methylene blue on hydrogenated ZnO nanoparticles. After ZnO is excited by the light with energy greater than its band gap, excited conduction band electrons and valence band holes are generated and migrate to the surface of ZnO. The photoelectrons react with oxygen when they reach the surface of ZnO nanoparticles to form superoxide

radical anions ($O_2^{\bullet -}$). The photoinduced holes react with surface hydroxyl to form reactive hydroxyl radicals ($OH^{\bullet}$). The superoxides and hydroxyl radicals then oxidize methylene blue eventually into CO_2, H_2O and other final compounds.[11f] As the surface chemical reactions normally occur on the time scale of milliseconds, most of the excited electrons and holes will recombine either in the bulk or on the surface of ZnO nanoparticles due to their short lifetimes (on the order of picoseconds to nanoseconds).[11g] This largely causes the low photocatalytic efficiency of ZnO nanoparticles. On the other hand, hydrogenated ZnO nanoparticles have larger amount of defect levels on the disordered surface along with possible hydrogen dopants resulted from the hydrogenation process. The localized defect states may enhance the charge separation in space.[1d] The trapped electrons and holes normally have extended lifetimes on the order of nanoseconds to milliseconds.[11g] This increases the charge transfer opportunities on the surface for the chemical reactions to decompose methylene blue molecules. Thus, the photocatalytic performance of hydrogenated ZnO nanoparticles is largely enhanced over pristine ZnO nanoparticles.

In a summary, we have demonstrated here that black ZnO nanoparticles can be obtained by hydrogenation treatment, and have displayed stable and better photocatalytic performance. This improvement was possibly due to the contributions from higher optical absorption, better charge separation benefited from disordered structure and more zinc vacancy defects created by hydrogenation.

Acknowledgements

X.C. acknowledges the support of this research from the College of Arts and Sciences, University of Missouri – Kansas City (UMKC), University of Missouri Research Board and the generous gift from Dow Kokam LLC.

Notes and references

1 (*a*) X. Chen, L. Liu, P. Y. Yu and S. S. Mao, *Science*, 2011, **331**, 746; (*b*) T. Xia and X. Chen, *J. Mater. Chem. A*, 2013, **1**, 2983; (*c*) X. Chen, L. Liu, Z. Liu, M. A. Marcus, W.-C. Wang, N. A. Oyler, M. E. Grass, B. Mao, P.-A. Glans, P. Y. Yu, J. Guo and S. S. Mao, *Sci. Rep.*, 2013, **3**, 1510; (*d*) L. Liu, P. P. Yu, X. Chen, S. S. Mao and D. Z. Shen, *Phys. Rev. Lett.*, 2013, **111**, 065505; (*e*) J. Lu, Y. Dai, H. Jin and B. Huang, *Phys. Chem. Chem. Phys.*, 2011, **13**, 18063; (*f*) G. Wang, H. Wang, Y. Ling, Y. Tang, X. Yang, R. C. Fitzmorris, C. Wang, J. Z. Zhang and Y. Li, *Nano Lett.*, 2011, **11**, 3026.

2 (*a*) A. Naldoni, S. Cappelli, C. L. Bianchi, R. Psaro and V. Dal Santo, *J. Am. Chem. Soc.*, 2012, **134**, 7600; (*b*) Z. Zheng, B. Huang, J. Lu, Z. Wang, X. Qin, X. Zhang, Y. Dai and M.-H. Whangbo, *Chem. Commun.*, 2012, **48**, 5733; (*c*) W. Wang, Y. Ni, C. Lu and Z. Xu, *RSC Adv.*, 2012, **2**, 8286; (*d*) Z. Wang, C. Yang, T. Lin, H. Yin, P. Chen, D. Wan, F. Xu, F. Huang, J. Lin, X. Xie and M. Jiang, *Adv. Funct. Mater.*, 2013, **23**, 5444; (*e*) H. Q. Lu, B. B. Zhao, R. L. Pan, J. F. Yao, L. Luo and Y. Liu, *RSC Adv.*, 2014, **4**, 1128; (*f*) H. Li, Z. H. Chen, C. K. Tsang, Z. Li, *et al.*, *J. Mater. Chem. A*, 2014, **2**, 229; (*g*) L. X. Zheng, H. Cheng, F. X. Liang, S. W. Shu, C. K. Tsang, H. Li, S. T. Lee and Y. Y. Li, *J. Phys. Chem. C*, 2012, **116**, 5509; (*h*) Z. Wang, C. Yang, T. Lin, H. Yin, P. Chen, D. Wan, F. Xu, F. Huang, J. Lin, X. Xie and M. Jiang, *Adv. Funct. Mater.*, 2013, **23**, 5444.

3 (*a*) J.-Y. Shin, J. H. Joo, D. Samuelis and J. Maier, *Chem. Mater.*, 2012, **24**, 543; (*b*) Z. Lu, C.-T. Yip, L. Wang, H. Huang and L. Zhou, *ChemPlusChem*, 2012, **77**, 991; (*c*) L. Shen, E. Uchaker, X. Zhang and G. Cao, *Adv. Mater.*, 2012, **24**, 6502; (*d*) T. Xia, W. Zhang, W. Li, N. A. Oyler, G. Liu and X. Chen, *Nano Energy*, 2013, **2**, 826; (*e*) G. Li, Z. Zhang, H. Peng and K. Chen, *RSC Adv.*, 2013, **3**, 11507.

4 (*a*) X. Lu, G. Wang, T. Zhai, M. Yu, J. Gan, Y. Tong and Y. Li, *Nano Lett.*, 2012, **12**, 1690; (*b*) C. Zhang, H. Yu, Y. Li, Y. Gao, Y. Zhao, W. Song, Z. Shao and B. Yi, *ChemSusChem*, 2013, **6**, 659; (*c*) W.-D. Zhu, C.-W. Wang, J.-B. Chen, D.-S. Li, F. Zhou and H.-L. Zhang, *Nanotechnology*, 2012, **23**, 455204; (*d*) T. Xia, C. Zhang, N. A. Oyler and X. Chen, *Adv. Mater.*, 2013, **25**, 6905.

5 (*a*) X. D. Wang, J. Song, J. Liu and Z. L. Wang, *Science*, 2007, **316**, 102; (*b*) Z. W. Pan, Z. R. Dai and Z. L. Wang, *Science*, 2001, **291**, 1947; (*c*) W. Wu, X. Wen and Z. L. Wang, *Science*, 2013, **340**, 952; (*d*) X. Yang, G. Zhu, S. Wang, R. Zhang, L. Lin, W. Z. Wu and Z. L. Wang, *Energy Environ. Sci.*, 2012, **5**, 9462; (*e*) Y. Liu, A. Das, S. Xu, Z. Lin, C. Xu, Z. L. Wang, A. Rohatgi and C. P. Wong, *Adv. Energy Mater.*, 2011, **2**, 47; (*f*) P. S. Hale, L. M. Maddox, J. G. Shapter, N. H. Voelcker, M. J. Ford and E. R. Waclawik, *J. Chem. Educ.*, 2005, **82**, 775; (*g*) S. Heidrun and A. Hans, *J. Appl. Crystallogr.*, 2006, **39**, 169.

6 (*a*) R. Jenkins and R. L. Snyder, *Introduction to X-ray Powder Diffractometry*, John Wiley & Sons Inc., New York, 1996; (*b*) T. Xia, N. Li, Y. Zhang, M. B. Kruger, J. Murowchick, A. Selloni and X. Chen, *ACS Appl. Mater. Interfaces*, 2013, **5**, 9883; (*c*) T. Xia, W. Zhang, J. Murowchick, G. Liu and X. Chen, *Nano Lett.*, 2013, **13**, 5289; (*d*) Y. Zhang, T. Xia, P. Wallenmeyer, C. X. Harris, A. A. Peterson, G. A. Corsiglia, J. Murowchick and X. Chen, *Energy Technol.*, 2014, **2**, 183.

7 (*a*) U. Diebold, *Surf. Sci. Rep.*, 2003, **48**, 53; (*b*) J. M. Pan, B. L. Maschhoff, U. Diebold and T. E. Madey, *J. Vac. Sci. Technol., A*, 1992, **10**, 2470; (*c*) C. A. Jenkins and D. M. Murphy, *J. Phys. Chem. B*, 1999, **103**, 1019; (*d*) J. Jun, M. Dhayal, J. H. Shin, J. C. Kim and N. Getoff, *Radiat. Phys. Chem.*, 2006, **75**, 583.

8 (*a*) C. G. Van de Walle, *Phys. Rev. Lett.*, 2000, **85**, 1012; (*b*) A. Janotti and C. G. Van de Walle, *Nat. Mater.*, 2007, **6**, 44; (*c*) D. Hofmann, A. Hofstaetter, F. Leiter, H. Zhou, F. Henecker, B. Meyer, S. Orlinskii, J. Schmidt and P. Baranov, *Phys. Rev. Lett.*, 2002, **88**, 045504; (*d*) X. Xue, T. Wang, X. Jiang, J. Jiang, C. Pan and Y. Wu, *CrystEngComm*, 2014, **16**, 1207.

9 (*a*) M. Rajalakshmi, A. K. Arora, B. S. Bendre and S. J. Mahamuni, *Appl. Phys.*, 2000, **87**, 2445; (*b*) T. Xia, W. Zhang, J. Murowchick, G. Liu and X. Chen, *Adv. Energy Mater.*, 2013, **3**, 1516.

10 (*a*) P. Jakes and E. Erdem, *Phys. Status Solidi RRL*, 2011, **5**, 56; (*b*) S. K. S. Parashar, B. S. Murty, S. Repp, S. Weber and E. Erdem, *J. Appl. Phys.*, 2012, **111**, 113712; (*c*) J. Lv, C. Li and J. J. BelBruno, *CrystEngComm*, 2013, **15**, 5620; (*d*) Z. Xia, Y. Wang, Y. Fang, Y. Wan, W. Xia and J. Sha, *J. Phys. Chem. C*, 2011, **115**, 14576.

11 (*a*) X. H. Wang, J. G. Li, H. Kamiyama, Y. Moriyoshi and T. Ishigaki, *J. Phys. Chem. B*, 2006, **110**, 6804; (*b*) X. Chen, S. Halasz, E. C. Giles, J. V. Mankus, J. C. Johnson and C. Burda, *J. Chem. Educ.*, 2006, **83**, 265; (*c*) Y. Mizukoshi, N. Ohtsu, S. Semboshi and N. Masahashi, *Appl. Catal., B*, 2009, **91**, 152; (*d*) X. Li, T. Xia, C. Xu, J. Murowchick and X. Chen, *Catal. Today*, 2014, **225**, 64; (*e*) T. Xia, Y. Zhang, J. Murowchick and X. Chen, *Catal. Today*, 2014, **225**, 2; (*f*) H. M. Xiong, D. G. Shchukin, H. Mohwald, Y. Xu and Y. Y. Xia, *Angew. Chem., Int. Ed.*, 2009, **48**, 2727; (*g*) M. R. Hoffmann, S. T. Martin, W. Choi and D. W. Bahnemann, *Chem. Rev.*, 1995, **95**, 69.

